NUMERICAL ANALYSIS OF THE OSCILLATORY BEHAVIORS OF SUPERSONIC IMPINGING JET FLOW

Sung In Kim, Seung O Park
Department of Aerospace Engineering, KAIST
373-1, Guseong-dong, Yuseong-gu, Daejeon, 305-701, Korea

Keywords: *supersonic impinging jet, oscillatory flow, self-sustained oscillation*

Abstract

Numerical simulations of supersonic impinging jet flows are carried out using the axisymmetric Navier-Stokes code. This paper focuses on the oscillatory flow features associated with the variation of the nozzle-to-plate distance. Frequencies of the surface pressure oscillation from computational results are found to be in accord with the measured impinging tones for various cases of nozzle-to-plate distance. The variation of this frequency with distance shows a staging behavior. The oscillatory behaviors of the flow structural changes and their characteristics are scrutinized.

1 Introduction

Supersonic jet flow impinging onto a flat plate is of practical importance in a number of engineering applications, of which the space or missile launch vehicle system is an example. An important problem in a supersonic impinging jet flow is that the jet of very high temperature and speed leads to a severe thermal and mechanical loading on the impinging plate. Supersonic impinging jet becomes oscillatory under certain operating conditions. The unsteady oscillation can make thermal and mechanical loading severer. Earlier researchers [1-5] have investigated the mean flow characteristics of this flow by using the Schilieren photography and the mean surface pressure measurement. These earlier studies elucidated many significant features of the flow. However, the data available in the earlier reports are limited mostly to mean flow properties.

Subsequent works have focused on unsteady flow oscillations and acoustic properties. One of the primary outcomes of these studies is that the highly unsteady, oscillatory nature of impinging jet, which is accompanied by discrete, high-amplitude acoustic tones referred to as impingement tones, is caused by a feedback loop. Powell [6] identified a feedback mechanism for self-sustained oscillations of the impinging jet flows. The energy of the feedback loop is provided by the instability waves in the shear layer of the jet. The downstream traveling vortical structures and the upstream propagating acoustic waves form the feedback loop.

It has been reported that the frequency of the impinging tone exhibits staging behavior as the nozzle-to-plate distance varies [6,7]. Krothapalli [7] obtained the near sound field microphone signal and surface pressure signal for a choked underexpanded impinging jet issuing from a rectangular nozzle of moderate pressure ratio. It was found that the frequencies of the dominant peak in both of sound and pressure signals coincide. Sakakibara and Iwamoto [8] carried out laminar Navier-Stokes computations of convergent nozzle impinging jet flows for various nozzle-to-plate distances. They showed that the frequency of the surface pressure oscillation exhibited staging behavior. Discrepancies between the frequencies of the impinging tone from measurement and of the surface pressure from their computation were identified, which was attributed to the grid problem. However, a detailed study of unsteady features of the flow structural change in the oscillatory impinging jet flow is rather rare.

The present study is concerned with the surface pressure oscillation and the oscillatory flow structural changes of axisymmetric supersonic jets from a converging choked nozzle at moderate nozzle pressure ratios. More specifically, we will focus on staging behavior of pressure oscillations for a given pressure ratio, with changing nozzle-to-plate distance. For these cases, we scrutinize the oscillatory behavior of the plate shock and the impinging region, which vary with the nozzle-to-plate distance. We then show how the pressure oscillatory features and the shock structural changes in each stage are distinguished.

2 Numerical Approach

We consider a unsteady laminar compressible flowfield governed by the following equations written in a cylindrical coordinate (x , r) system:

$$\frac{\partial Q}{\partial t}+\frac{\partial E}{\partial x}+\frac{\partial F}{\partial r}+G=\frac{\partial E_v}{\partial x}+\frac{\partial F_v}{\partial r}+G_v \qquad (1)$$

where $Q=\left[\rho,\rho u,\rho v,\rho e_t\right]^{\mathrm{T}}$ is the vector of conserved variables, E,F,G are the inviscid flux vectors and E_v,F_v,G_v are the viscous flux vectors.

The variables are normalized by the nozzle exit properties; Length by the nozzle exit diameter, D, velocity by the speed of sound, c_e, pressure by $\rho_e c_e^2$, time by D/c_e, and viscosity by μ_e. We assume that the gas is perfect. The molecular viscosity is calculated using the Sutherland's law.

$$\left[\frac{1}{J\Delta t}+\frac{\vartheta}{1+\varphi}\left(\frac{\partial R(Q^p)}{\partial Q}\right)\right]\left(Q^{p+1}-Q^p\right) \qquad (2)$$
$$=-\frac{1}{1+\varphi}R(Q^p)$$
$$-\frac{1}{J\Delta t}\left[Q^p-\frac{1+2\varphi}{1+\varphi}Q^n+\frac{\varphi}{1+\varphi}Q^{n-1}\right]$$

For time accurate calculation, we adopt the subiteration time advance scheme of Pulliam [9], which is formulated as Eq. (2), where Q^p and Q^{p+1} are the solutions of subiteration level, and Q^n and Q^{n-1} are the solutions of previous time levels. The solution at time level $n+1$ is given by the converged solution Q^{p+1}. In this study, we take $\vartheta=1$ and $\varphi=1/2$, which gives the three point backward implicit scheme to result in the second order accuracy in time. The MLDFSS (Modified Low-Diffusion Flux-Splitting Scheme), adopted in Lee & Park [10], is used to evaluate the inviscid fluxes on the cell surfaces. Central difference is used to calculate viscous terms. For the calculation of Jacobian matrices, $\partial R/\partial Q$, in the implicit part (left hand side) of Eq. (2), we use Steger-Warming's flux vector splitting scheme for inviscid fluxes, and retain only non-mixd derivative terms for viscous fluxes. To solve the discretized equations, we adopt the point symmetric Gauss-Seidel (point SGS) scheme.

We consider axisymmetric supersonic impinging jet flows driven by the sonic flow of a convergent nozzle as sketched in Fig. 1. The nozzle exit diameter D is 10mm. The ambient air temperature T_a and the static pressure P_a are 288.15 K and 1atm, respectively. In the present computation, we assume that the choked sonic flow condition is achieved at the nozzle exit. Thus the inlet boundary of this computation is the nozzle exit where the pressure, the velocity and the temperature are fixed from the isentropic relations. No slip and adiabatic wall boundary conditions have been used for the nozzle wall and the impinging flat plate. The first order extrapolation is applied on the far field free boundaries.

A multi-block system of structured grids is used. Grid points are clustered near the wall and the jet plume region. Tests are conducted to select a suitable grid, which can capture the salient features of flow oscillation. Surface pressure oscillations at several radial locations and the shock cell structures are compared for the different grid systems. The computation is carried out till about $200D/V_e$ (V_e: the nozzle exit velocity). A self-sustained oscillatory state

is found to be reached after $t \approx 100D/V_e$. Beyond this time, the frequency of oscillations becomes a constant value. As a result of grid tests, the grid of $\Delta x_{\min} = \Delta r_{\min} = 0.001D$, $\Delta x_{\max} = 0.013D$, $\Delta r_{\max} = 0.0114D$ is sufficient to capture the oscillatory features of the flow. We recall here that Sakakibara and Iwamoto [8] used the grid of $\Delta x_{\min} \cong 0.01D$ and $\Delta r_{\min} \cong 0.01D$. Hence the present grid system is far denser than theirs. Choice of time step is an important factor in unsteady flow analysis. By scrutinizing the pressure oscillation patterns including the amplitude and the time period of the oscillation, we have found that $\Delta t = 0.003D/V_e$ is sufficient for unsteady analysis.

3 Results and Discussion

For impinging supersonic jet flows, one of important operating parameters that affect the flow characteristic is the distance from the nozzle exit to the impinging plate (H). Therefore, the flow structural changes and the oscillatory features of surface pressure in impinging jet flows are investigated by varying the distance from the nozzle to the plate (H) for a given pressure ratio. The distance to the impinging plate is varied from 2.0 times to 3.0 times the nozzle exit diameter (H/D=2.0 ~ 3.0) with the nozzle pressure ratio fixed at P_0/P_a=3.0 (P_0: the stagnation chamber pressure). In this case, the nozzle exit pressure is 1.605 times larger than the ambient pressure. Thus the jet is in an underexpanded condition. The jet issuing from the nozzle exit undergoes expansion and compression cycles repeatedly to adapt to the ambient pressure. However, the shock cell structures are disturbed by the impingement and hence exhibit periodic structural changes accompanying pressure oscillation.

3.1 Surface Pressure Oscillations

To characterize the features of surface pressure oscillation, power spectra of the pressure signals have been calculated. The frequencies of the pressure oscillations at the center (r/D=0.0) of the plate for various nozzle-to-plate distance ratios (H/D) are shown in Fig. 2. For the comparison with the acoustical measurement, the frequencies of the impinging tones from the measurements [6,8] are also contained in Fig. 2. Powell [6] found that the impinging tones, referred to the principal tones, formed a sawtooth pattern with seven possible stages (labeled II through VIII) for the range of H/D=0.5~7.0. Some separate tones did occur; these had the same general slope as did the principal tones. These were called upper secondary tones in that they are not an integral part of the dominant pattern. The traveling time of disturbance increases as the geometrical length of the feedback loop lengthens due to the increase of the nozzle-to-plate distance. Thus, within a specific range of staging behavior the frequency of oscillation decreases as the distance increases, as shown in Fig. 2. Figure 2 clearly indicates that the frequency changes with a jump at a certain distance (H/D) known as staging behavior. It is not yet clearly understood why this staging behavior occurs. Figure 2 also shows that the frequencies of the surface pressure oscillation are in good accord with the impinging tones. In the present computation for the range of H/D=2.0~3.0, two stages labeled IV-V and the upper secondary frequencies (the cases of H/D=2.0 and 2.1) have been observed.

Figure 3 gives several time histories of pressure variation at the center of the impinging plate for various distances (H/D), when the flow is in self-sustained periodic oscillation. The surface pressure oscillations of the cases of H/D=2.2~2.5 in stage IV show similar patterns. However, the pressure oscillation of the case of H/D=2.6 in stage V has a different pattern from the case of H/D=2.5 in stage IV. The frequency of surface pressure oscillation increases abruptly to higher frequency, while the maximum pressure and the amplitude of oscillation ($P_{\max}/P_0 \simeq 0.98$, $\Delta P/P_0 \simeq 0.22$ for H/D=2.6) suddenly drops to about half of the amplitude of H/D=2.5 case ($P_{\max}/P_0 \simeq 1.16$, $\Delta P/P_0 \simeq 0.44$). For flows where $2.6 \le \mathrm{H/D} \le 3.0$, the pressure

oscillations follow a similar pattern. However, the amplitude of surface pressure oscillation increases and the frequency of oscillation decreases with the nozzle-to-plate distance.

3.2 Flow Structures

Surface pressure oscillations seen in Fig. 3 reflect flow pattern changes during a oscillation period. To examine this in detail, we first illustrate the surface center pressure history and the variation of the plate shock position on the jet axis in Fig. 4. The frequencies of pressure oscillation of H/D=2.5 and 2.6 are 18.22 kHz and 22.15 kHz, respectively. The abscissa is a time normalized by the oscillation period, T, which is about 54.9μsec for H/D=2.5 and 45.1μsec for H/D=2.6. The ordinates are the pressure nondimensionalized by the stagnation chamber pressure on one side, and the plate shock position, X_S, measured from the plate to the plate shock normalized by the nozzle exit diameter on the other side.

When a supersonic jet flow impinges perpendicularly on a flat plate, a strong normal shock, known as 'plate shock' or 'standoff shock', occurs over the plate. In the oscillatory impinging jet flows, the plate shock also oscillates along the jet axis, and the frequencies of the plate shock oscillation are identical with those of the surface pressure oscillation. Figure 4 shows that the surface pressure increases when the plate shock moves toward the wall, and vice versa. However, the uppermost position of the plate shock does no necessarily imply the lowest surface pressure, suggesting that a very complex flow structure may exist near the wall. Figures 5 and 6 contain snapshots of instantaneous streamlines and iso-pressure contours at several instants associated with Fig. 4. The flow patterns shown in Figs. 5 and 6 appear periodically with the period of T.

To aid in understanding these instantaneous flow patterns, we present static pressure variations along the jet centerline in Fig. 7. From Fig. 7 and also from Figs. 5 and 6, we find that the first cell from the nozzle characterized by expansion and monotonic decrease in pressure does not vary much with time. The flow pattern of the major portion of first cell remains almost the same at all times. This first expansion cell is followed by a shock. As evidenced in Fig. 7, this compression region and the region downstream of this shock are seen to undergo significant changes with time. This dramatic and diverse change of jet flow pattern seems to be strongly associated with the shear layer between the supersonic jet and the entrained ambient flow. For example, the pressure distributions 2 and 8 of Fig. 7(a) are very much different each other. The streamlines and iso-pressure contours corresponding to these instants of Fig. 5(b) and 5(h) show that the shear layer structures are very much different each other. As another example case, let us compare the pressure curves 3 and 9 from Fig. 7(b) and the corresponding flow patterns of Fig. 6(c) and 6(i). We again see that the shear layer structures for these two instants are quite different each other. In fact, it is not difficult to note that the iso-pressure contours including the shock wave structures are of similar type if the corresponding shear layer structures are similar. Of most notable difference of Figs. 5 and 6 is that the three vortical structures prevail if Fig. 6 (the case of H/D=2.6 in stage V), while the two vortical structures are dominant in Fig. 5 (the case of H/D=2.5 in stage IV). It is not yet clear, whether this will distinguish the staging behavior and thus needs further investigation.

4 Conclusion

Computational study on the unsteady supersonic impinging jet flow has been carried out. Oscillatory behavior of underexpanded supersonic jets issuing from the convergent sonic nozzle has been investigated by varying the nozzle-to-plate distance at a fixed nozzle pressure ratio. It has been found that the frequency variation of the surface pressure oscillation is in accord with the frequency of impinging tone, which shows a staging behavior as the distance increases

Flow structures and pressure distributions at various instants are presented from different

stages to illustrate how they differ each other. These flow patterns clearly indicate that the behavior of the shear layer between the supersonic jet and the ambient fluid and the behavior of main jet structural change are strongly coupled together. To understand well the staging behavior, the relationship between the flow structural changes and the changes of the jet shear layer structures, which provides the energy of the feedback loop, is to be investigated more carefully.

References

[1] Donaldson, C. D. and Snedeker, R. S. A study of free jet impingement. Part 1. Mean properties of free and impinging jets. *J. Fluid Mech.*, Vol. 45, pp 281-319, 1971.

[2] Ginzberg, I. P., Semilentenko, B. G., Terpigorev, V. S. and Uskov, V. N. Some singularities of supersonic underexpanded jet interaction with a plane obstacle. *J. Eng. Phys.*, Vol. 19, pp 1081-1084, 1973.

[3] Carling, J. C. and Hunt, B. L. The near wall jet of a normally impinging, uniform, axisymmetric, supersonic jet. *J. Fluid Mech.*, Vol. 66, pp 159-176, 1974.

[4] Kalghatgi, G. T. and Hunt, B. L. The occurrence of stagnation bubbles in supersonic jet impingement flows. *Aero. Quart.*, Vol. 27, pp 169-185, 1976.

[5] Lamont, P. J. and Hunt, B. L. The impingement of underexpanded axisymmetric jets on perpendicular and inclined flat plates. *J. Fluid Mech.*, Vol. 100, pp 471-511, 1980.

[6] Powell, A. The sound-producing oscillations of round underexpanded jets impinging on normal plates. *J. Acoust. Soc. Am.*, Vol. 83, pp 515-533, 1988.

[7] Krothapalli, A. Discrete tones generated by an impinging underexpanded rectangular jet. *AIAA J.*, Vol. 23, pp 1910-1915, 1985.

[8] Sakakibara, Y. and Iwamoto, J. Numerical study of oscillation mechanism in underexpanded jet impinging on plate. *J. Fluids Eng.*, Vol. 120, pp 477-481, 1998.

[9] Pulliam, T. H. Time accuracy and the use of implicit methods. AIAA Paper 93-3360, 1993.

[10] Lee, C. H. and Park, S. O. Computations of hypersonic flows over blunt body using a modified low-diffusion flux-splitting scheme. *CFD J.*, Vol. 10, pp 490-500, 2002.

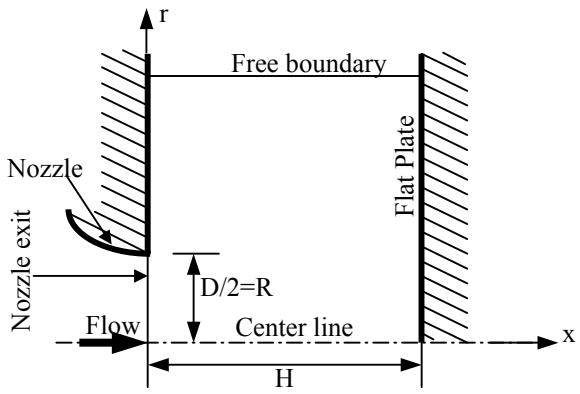

Fig. 1. Computational flow model and boundary conditions

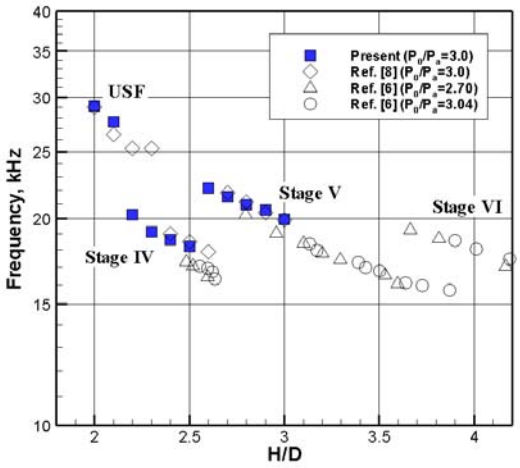

Fig. 2. Frequency of the pressure oscillation and the impinging tones versus distance.
(USF stands for upper secondary frequency)

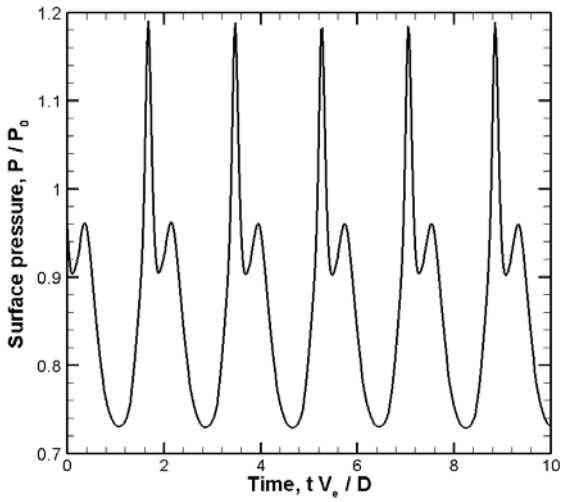

(a) H/D = 2.3 in Stage IV

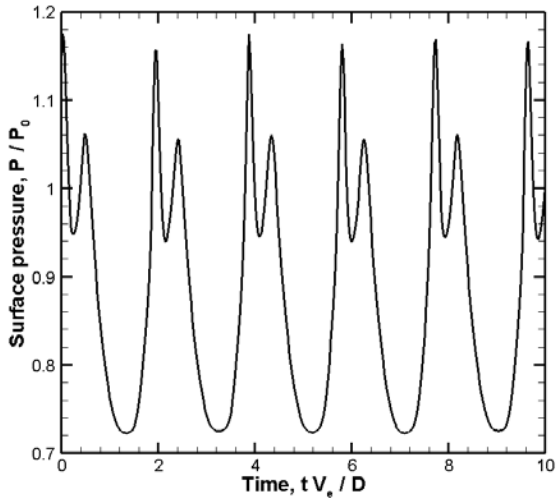

(b) H/D = 2.5 in Stage IV

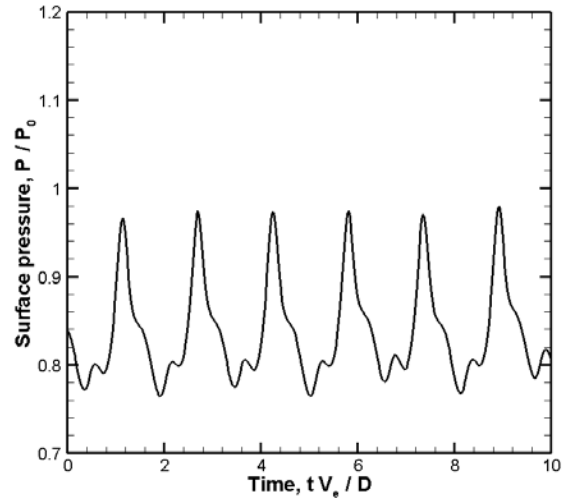

(c) H/D = 2.6 in Stage V

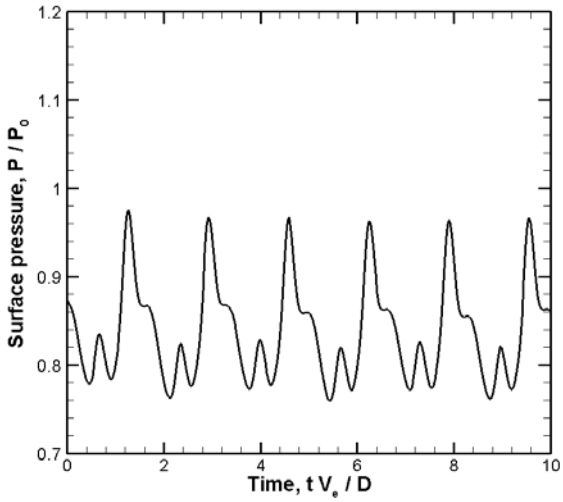

(d) H/D = 2.8 in Stage V

Fig. 3. Surface pressure time histories at the center of the plate for various H/D, P_0/P_a =3.0.

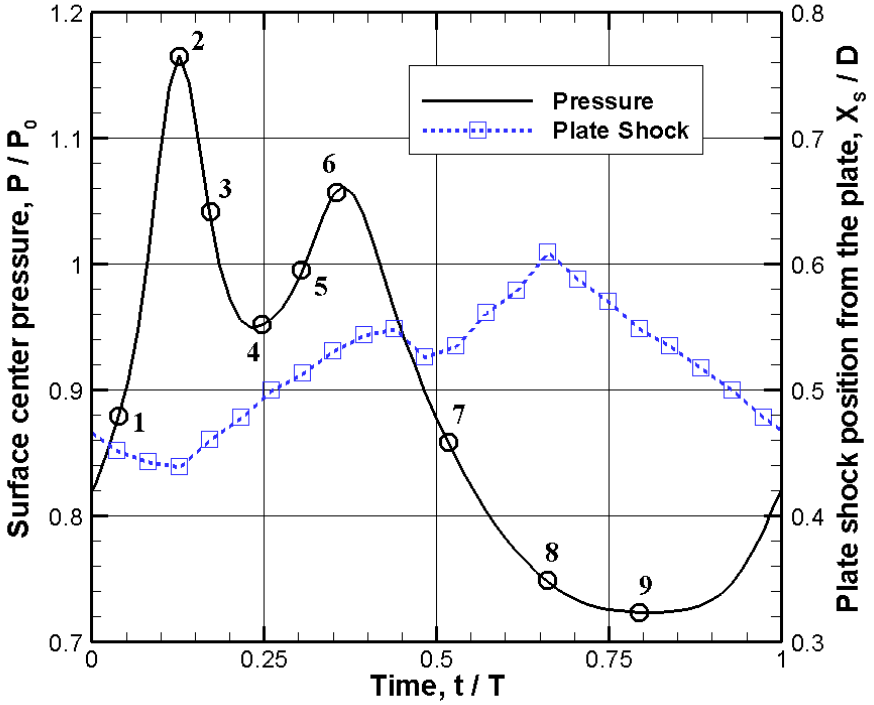

(a) At H/D=2.5 in Stage IV

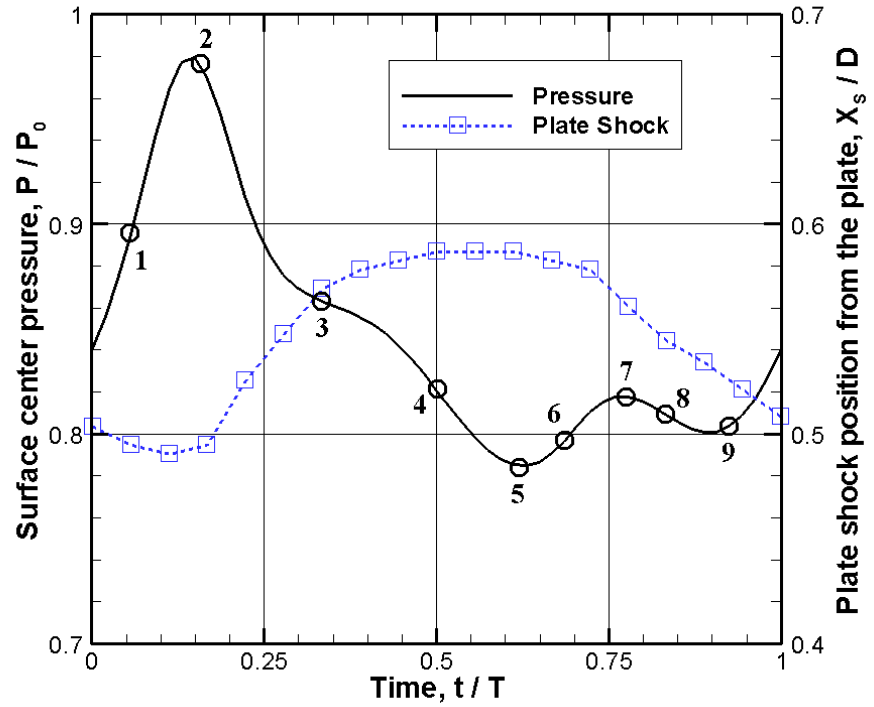

(b) At H/D=2.6 in Stage V

Fig. 4. Surface center pressure time histories and the plate shock position.
(T : the period time of surface pressure oscillation)

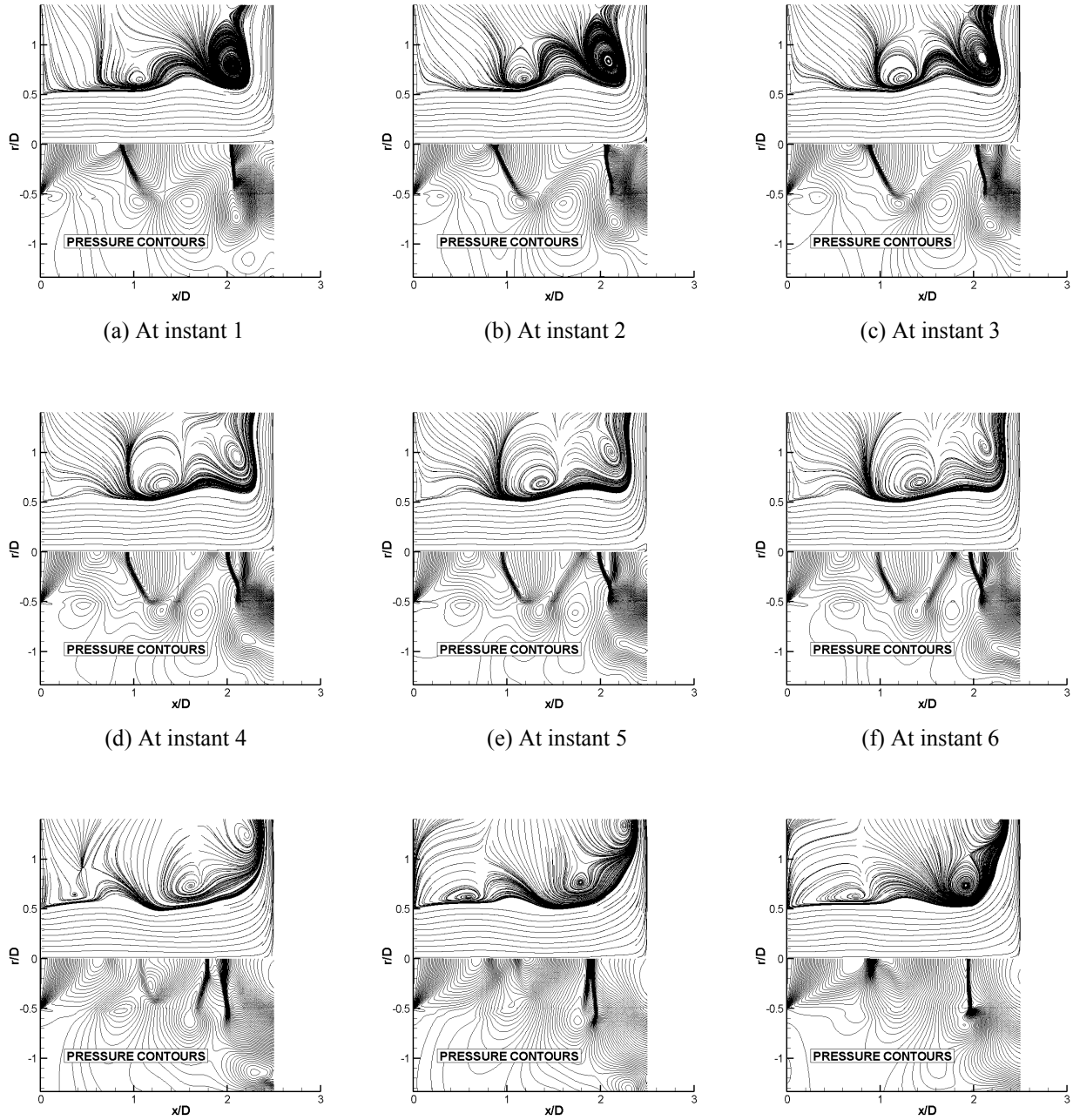

(a) At instant 1 (b) At instant 2 (c) At instant 3

(d) At instant 4 (e) At instant 5 (f) At instant 6

(g) At instant 7 (h) At instant 8 (i) At instant 9

Fig. 5. Instantaneous flow patterns in a cycle of oscillation, H/D=2.5, P_0/P_a =3.0.

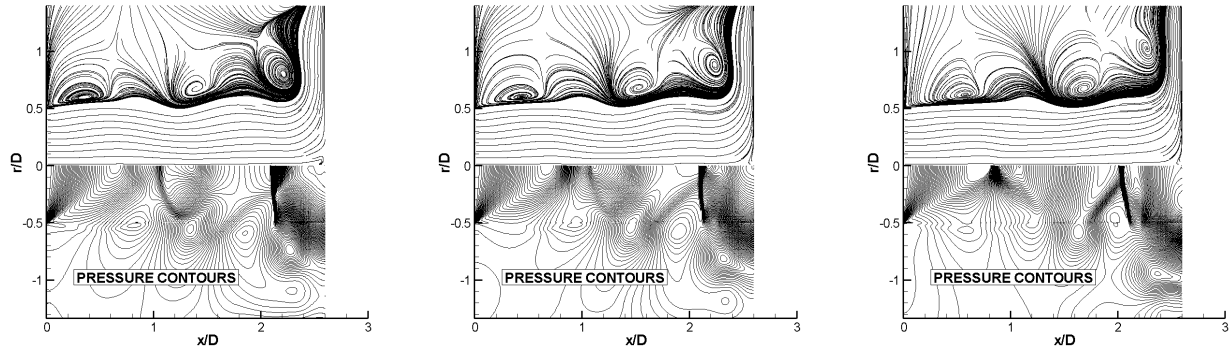

(a) At instant 1 (b) At instant 2 (c) At instant 3

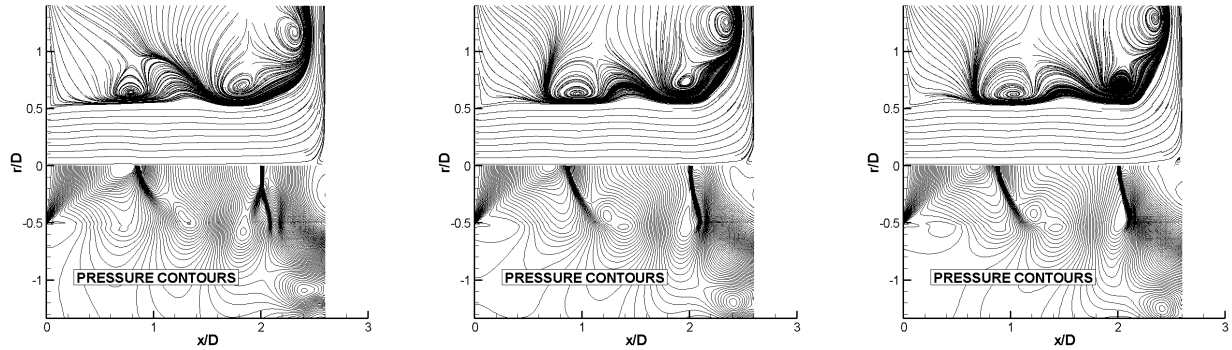

(d) At instant 4 (e) At instant 5 (f) At instant 6

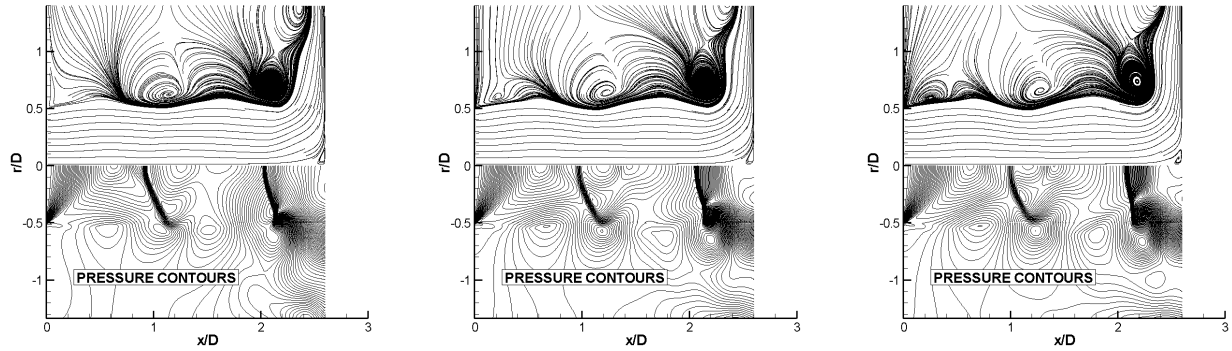

(g) At instant 7 (h) At instant 8 (i) At instant 9

Fig. 6. Instantaneous flow patterns in a cycle of oscillation, H/D=2.6, P_0/P_a =3.0.

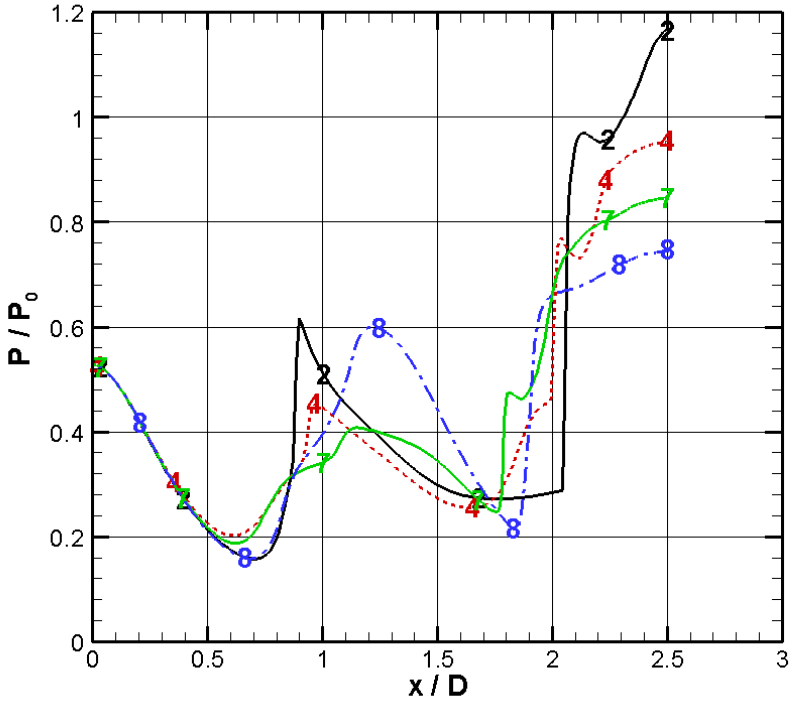

(a) At H/D=2.5 in Stage IV

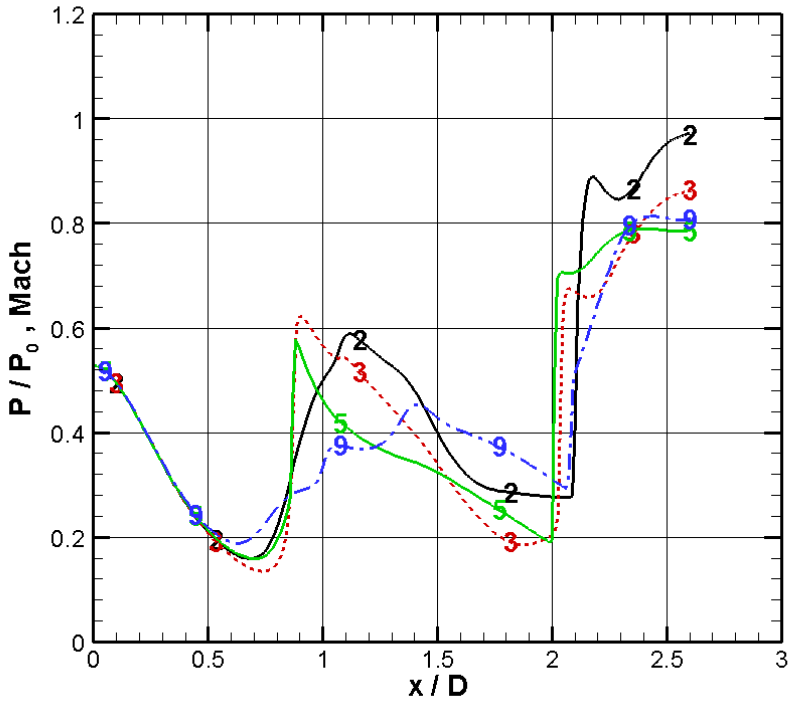

(b) At H/D=2.6 in Stage IV

Fig. 7. Instantaneous pressure distributions along the jet axis.